

The Laminar Nonisothermal Flow of Non-Newtonian Fluids

RICHARD W. HANKS and ERNEST B. CHRISTIANSEN

University of Utah, Salt Lake City, Utah

The equations which describe the process of simultaneous heat and momentum transport are solved to obtain the pressure loss-flow rate relation for the laminar flow of pseudoplastic liquids through a smooth heated pipe. The rheology of the liquids is characterized by a temperature-reduced form of the empirical Ostwald-deWaele or power law equation.

Two solutions to the basic equations are presented, a numerical integration of the heat conduction differential equation and an approximate solution based upon a simplified model of the temperature profile.

Experimental data obtained with eighteen different pseudoplastic solutions and the limited data available from the literature are compared with theoretical predictions and are correlated over a 5,000-fold range of friction factors and pseudoplastic Reynolds numbers with a standard deviation of 4.9%.

PREVIOUS RESEARCH

The mathematical analysis of simultaneous heat and momentum transport in the laminar flow of fluids results in five scalar partial differential equations which must be satisfied simultaneously. Some of these equations are nonlinear, and no general analytic solutions are known. Various investigators (1, 2, 3, 4, 5) have solved the equations for certain restricted cases. Over moderate ranges of experimental conditions their results are adequate, but none of the extant analytical solutions is sufficient for the enormous ranges of variables which have been examined experimentally. The analytical approaches are inadequate when large radial and/or axial temperature gradients exist.

Sieder and Tate (6) and others (7, 8) have determined the pressure drop-flow rate relation for highly nonisothermal Newtonian flow by empirical methods. This approach has proved useful in the design of heating and cooling equipment, as it has facilitated the estimation of nonisothermal pressure losses and hence the rational sizing of pumps and estimation of energy costs. No adequate method for predicting pressure losses through heaters or coolers is known for non-Newtonian flow.

THEORETICAL ANALYSIS

The simultaneous transport of heat and momentum is describable in terms of the hydrodynamic equations of motion, continuity, and energy conservation. In general notation these equations are

Equation of motion:

$$\rho \frac{D\bar{u}}{Dt} = \bar{F}_b + \nabla \cdot \bar{T}$$

Equation of continuity:

$$-\frac{\partial \rho}{\partial t} = \nabla \cdot \rho \bar{u}$$

Energy equation:

$$c_p \frac{DT}{Dt} = \nabla \cdot (k \nabla T) + \bar{T} : \nabla \bar{u}$$

In non-Newtonian flow problems the complex relation between the stress tensor and the strain-rate tensor often leads to intractable equations. In order to avoid this complication the authors introduce the following assumptions to simplify the general equations:

1. The fluid is incompressible and has temperature independent heat capacity and thermal conductivity.
2. The flow is steady ($\partial/\partial t \equiv 0$).
3. The flow channel is cylindrical.
4. The flow field is axially symmetric ($\partial/\partial \phi \equiv 0$).
5. Body forces are unimportant ($\bar{F}_b = 0$).
6. The energy dissipated by viscous shear is negligible in comparison with that transported by thermal conduction ($\bar{T} : \nabla \bar{u} \dot{=} 0$).
7. Radial and angular flow is negligible compared with axial flow ($v = w = 0$; $\bar{u} = \bar{u}$).
8. The pressure gradient is a function only of the axial coordinate ($\partial p/\partial r = 0$).

9. Conduction in the axial direction is negligible in comparison with that in the radial direction ($\partial^2 T/\partial z^2 = 0$).

10. Shear stress is a function only of radius [$\tau_{rz} = \tau(r)$].

Upon introduction of assumptions 1 to 4, 6, 7, and 9 the energy equation is reduced to

$$u \frac{\partial T}{\partial z} = \frac{k}{\rho c} \left\{ \frac{\partial^2 T}{\partial r^2} + \frac{1}{r} \frac{\partial T}{\partial r} \right\} \quad (1)$$

In order to solve Equation (1) one must know the velocity distribution u as a function of r and z . This may be ascertained from the equations of motion and continuity coupled with a rheological stress-strain rate relation.

The rheological equation chosen is the simple empirical Ostwald-deWaele or power law equation modified to include temperature effects (9, 10):

$$\tau = k_s \dot{S}_r^n \quad (2)$$

where \dot{S}_r is given by

$$\dot{S}_r = \left(-\frac{\partial u}{\partial r} \right) \exp \{E^\ddagger/RT\} \quad (3)$$

The parameter E^\ddagger is an experimental energy of activation which is determined from rheological data obtained at different temperatures; k_s is the unit shear-rate value of τ (somewhat analogous to a viscosity), and n is the slope of a logarithmic plot of τ vs. \dot{S}_r ; E^\ddagger , k_s , and n will be considered as constants in the following analysis.

Introduction of the above assumptions into the equations of motion and continuity or a force balance written for a cylindrical fluid element results

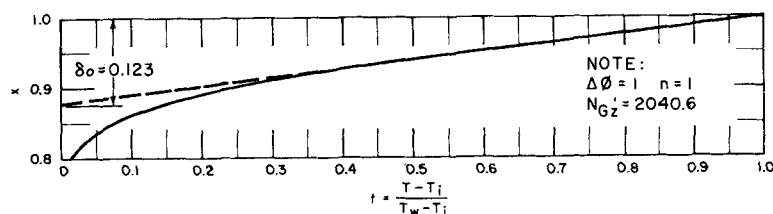


Fig. 1. Enlarged temperature-profile curve.

R. W. Hanks is with Union Carbide Nuclear Company, Oak Ridge Gaseous Diffusion Plant, Oak Ridge, Tennessee.

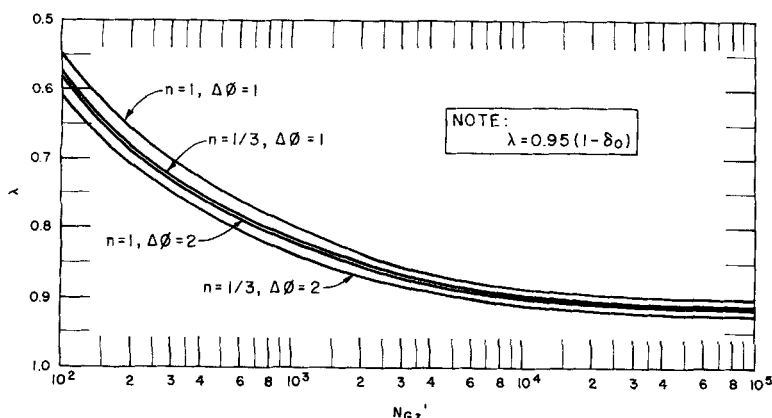


Fig. 2. Nonisothermal laminar-flow parameter λ .

in the following form of the equation of motion:

$$\frac{1}{r} \frac{d}{dr} (r\tau) = dp/dz$$

which, upon integration with the condition that $\tau(r=0)$ be finite, results in the familiar expression

$$\tau = \frac{1}{2} r \left(\frac{-\Delta p}{L} \right) = \frac{r}{R_w} \tau_w \quad (4)$$

where the authors have used assumptions 8 and 10 above, which show that $\partial p/\partial z$ can at most be a constant equal to $-\Delta p/L$. The validity of assumption 8 and the equation of dp/dz with $-\Delta p/L$ was borne out by limited experimental observations which indicated the variation of Δp with length to be less than 2%. The real justification for these assumptions is found in the excellence of the final correlation derived therefrom.

It is convenient to introduce the dimensionless coordinate $x = r/R_w$ which varies between the limits zero and unity at the center line and wall of the tube. Equation (2) may be rewritten as

$$\left(-\frac{\partial u}{\partial x} \right) = R_w (\tau_w/k_s)^{1/n} (x^{1/n}) \exp[-\phi(x,z)] \quad (5)$$

where

$$\phi(x,z) \equiv E^\ddagger/RT(x,z) \quad (6)$$

and $T(x,z)$ is the temperature distribution.

Equation (5) may be used to derive the expression

$$\Gamma \equiv \frac{Q}{\pi R_w^3} = 2[\tau_w/k_s \exp(n\phi_i)]^{1/n} \int_0^1 x \int_x^1 (x^{1/n}) \exp[\phi_i - \phi(x,z)] dx dx \quad (7)$$

where $\phi_i = E^\ddagger/RT_i$ and Q is the volumetric flow rate. Upon introduction of the identity

$$k_s = k_o [(1+3n)/n]^n \quad (8)$$

Equation (7) becomes

$$\tau_w = k_{\gamma i} \Gamma^n \zeta_f^{-n} \quad (9)$$

where

$$\zeta_f \equiv 2[(1+3n)/n] \int_0^1 x \int_x^1 (x^{1/n}) \exp[\phi_i - \phi(x,z)] dx dx \quad (10)$$

and

$$k_{\gamma i} \equiv k_s \exp(n\phi_i) \quad (11)$$

The constant k_s is the unit Γ , intercept of a logarithmic plot of τ_w vs. Γ , $\Gamma \equiv \Gamma \exp(E^\ddagger/RT)$. Equation (8) is derived from Equation (5) with $\phi(x,z) = \phi_i$

by obtaining the expression for Γ and then transforming it into the form $\tau_w = k(n)\Gamma^n$.

Upon introduction of the Fanning friction factor defined as

$$f \equiv \frac{g_c \rho D \Delta p}{2G^2 L} = 2g_c \tau_w / \rho \bar{v}^2 \quad (12)$$

where $G = \rho \bar{v}$ and \bar{v} is the area mean velocity

$$\bar{v} \equiv Q/\pi R_w^2 = \frac{1}{2} D \Gamma \quad (13)$$

Equation (9) is reduced to the dimensionless form

$$f_{ni} = \frac{16}{2\rho D^2 \Gamma^{2-n}} \frac{\zeta_f^n}{g_c k_{\gamma i}} \quad (14)$$

For isothermal flow $\zeta_f = 1$ and Equation (14) is reduced to

$$f_{iso} = \frac{16}{2\rho D^2 \Gamma^{2-n}} \frac{1}{g_c k_{\gamma i}} \quad (15)$$

If common terms are eliminated between Equations (14) and (15), and the condition $\Gamma_{iso} = \Gamma_{ni}$ imposed, then

$$f_{ni} = f_{iso} \zeta_f^{-n} \quad (16)$$

where

$$f_{iso} = 16 N_{Rei}^{-1} \quad (17)$$

and

$$N_{Rei} \equiv \frac{2\rho D^2 \Gamma^{2-n}}{g_c k_{\gamma i}} \quad (18)$$

The friction factor f_{iso} is that friction factor which would be observed if the fluid were flowing isothermally with the same average linear velocity as that existing in the nonisothermal flow.

Equation (17) is a form (11, 12, 13) of the Poiseuille equation for fluids conforming rheologically to Equation (2). Other investigators (11) have presented results which, for the case considered here, may readily be shown (12) to reduce to Equation (17).

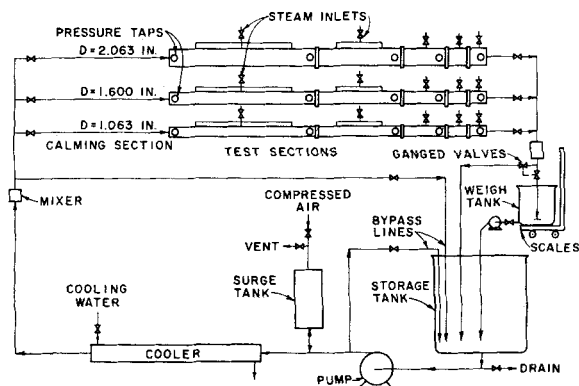


Fig. 3. Equipment flow sheet.

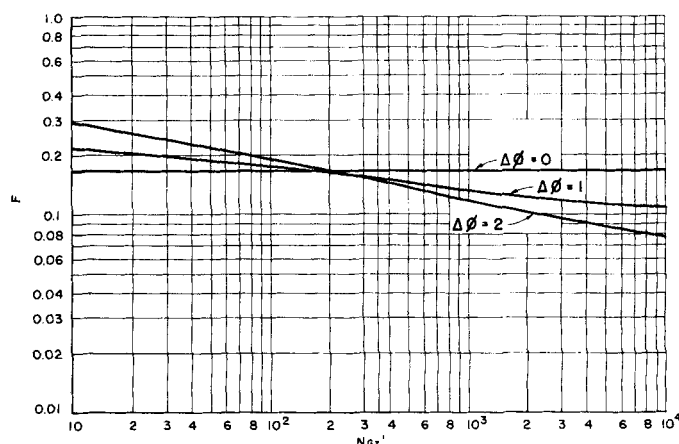


Fig. 4. Computer curves for $n = 1/3$.

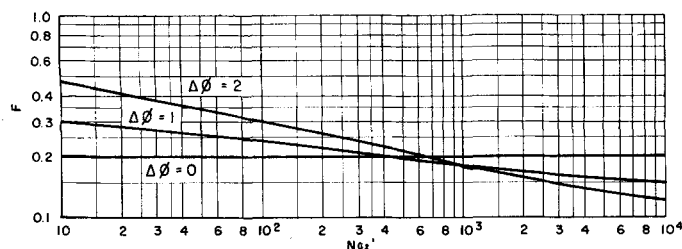


Fig. 5. Computer curves for $n = 1/2$.

In order for Equation (16) to be useful one must solve Equation (10). Two alternatives are available, numerical integration of the energy equation or the invention of a model of the temperature profile from which an approximate solution may be derived. These approaches will be discussed in the order mentioned.

NUMERICAL INTEGRATION OF ENERGY EQUATION

Equation (5) may be integrated once with respect to radius to give the velocity distribution

$$u(x, z) = R_w (\tau_w/k_s)^{1/n} \int_x^1 (x^{1/n}) \exp[-\phi(x, z)] dx \quad (19)$$

Multiplying Equation (7) by $\rho\pi R_w^3$ one gets the mass flow rate

$$w = 2\pi R_w^3 \rho (\tau_w/k_s)^{1/n} \int_0^1 x \int_x^1 (x^{1/n}) \exp[-\phi(x, z)] dx dx \quad (20)$$

Elimination of the quantity $(\tau_w/k_s)^{1/n}$ between Equations (19) and (20) and multiplication of the result by $\exp(\phi_w)/\exp(\phi_w)$ leads to

$$u(x, z) = \frac{w}{2\pi\rho R_w^2} \frac{I_1}{I_2} \quad (21)$$

where

$$I_1 = \int_x^1 (x^{1/n}) \exp[\phi_w - \phi(x, z)] dx \quad (22)$$

and

$$I_2 = \int_0^1 x I_1 dx \quad (23)$$

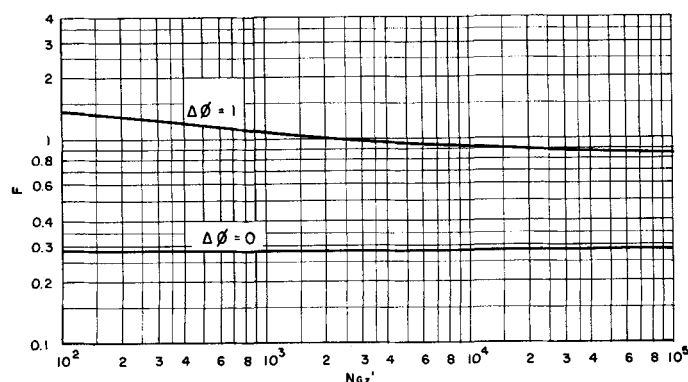


Fig. 6. Computer curves for $n = 2$.

If Equation (21) is introduced into Equation (1), one has

$$\frac{\partial T}{\partial z} = \frac{2\pi k}{wc} \frac{I_2}{I_1} \left\{ \frac{\partial^2 T}{\partial x^2} + \frac{1}{x} \frac{\partial T}{\partial x} \right\} \quad (24)$$

which is the partial differential equation to be integrated numerically.

The function ζ , defined by Equation (10) may be calculated from

$$\zeta_r = \frac{1 + 3n}{n} \exp[(1 - n)\Delta\phi] F \quad (25)$$

where

$$F = 2I_2 \exp(n\Delta\phi) \quad (26)$$

and

$$\Delta\phi \equiv \frac{E^+}{R} \left[\frac{1}{T_i} - \frac{1}{T_w} \right] \quad (27)$$

The quantity F is the parameter actually computed in the numerical integration of Equation (24). Equation (25), together with Figures 4, 5, and 6, permits the calculation of ζ , as determined by numerical integration. The velocity profile may also be computed directly by using the incremental solutions of I_1 obtained in the numerical integration process.

The numerical integration of Equation (24) was accomplished by standard techniques (9, 12, 14) with the aid of a digital computer. Integrations were performed for the cases shown in Table 1.

APPROXIMATE SOLUTION

The function ζ , may be obtained in algebraic form if a mathematically

tractable function $\exp[\phi_i - \phi(x, z)]$ is known. For this purpose it is convenient to construct a simplified model of the temperature profile.

If the temperature profiles obtained by the numerical integration discussed above are used to calculate $\phi(x, z)$ for a given set of parameters n and $\Delta\phi$, a family of curves is obtained. These curves are parameterized by a modified Graetz number, $N'_{Gz} \equiv wc/kL = \pi R_w^2 N_{Gz}/L^2$. These curves suggest, as a model, the division of the profile into two parts, one a constant and the other a tractable function, of x and z . The function chosen is

$$\phi(x, z) = \phi_i = \text{const.}; 0 \leq x \leq \lambda(z) \quad (28)$$

$$\phi(x, z) = \phi_w + \Delta\phi \ln x / \ln \lambda(z);$$

$$\lambda(z) \leq x \leq 1 \quad (29)$$

where $\lambda(z)$ is a function to be determined from the temperature profile curves computed above. The curve in Figure 1 is the upper portion of one such curve for fixed values of N'_{Gz} , n , and $\Delta\phi$. For $t \geq 0.5$ the curve is essentially linear. When this linear portion is extrapolated to the $t = 0$ axis, as illustrated in Figure 1, an intercept $x_0 = 1 - \delta_0$ is obtained. The function $\lambda(z)$ is defined as

$$\lambda(z) = \alpha(1 - \delta_0) \quad (30)$$

where α is a numerical parameter to be determined experimentally. A value of 0.95 for α was found to be sufficient. In Figure 2 is shown a plot of $\lambda(z)$ vs. N'_{Gz} . The curves shown were determined from the computed temperature profiles by the above method with $\alpha = 0.95$.

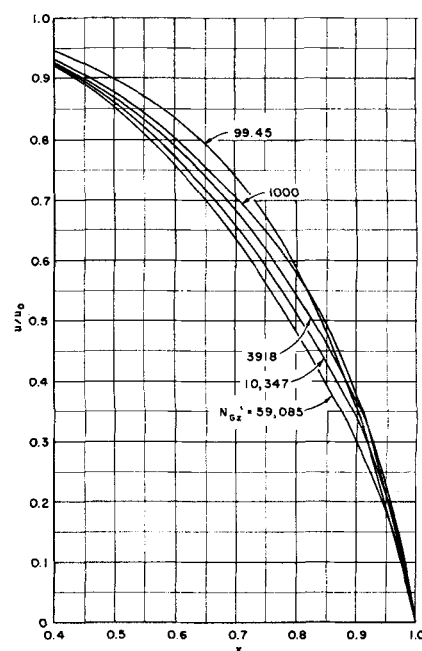


Fig. 7. Computed velocity profiles.

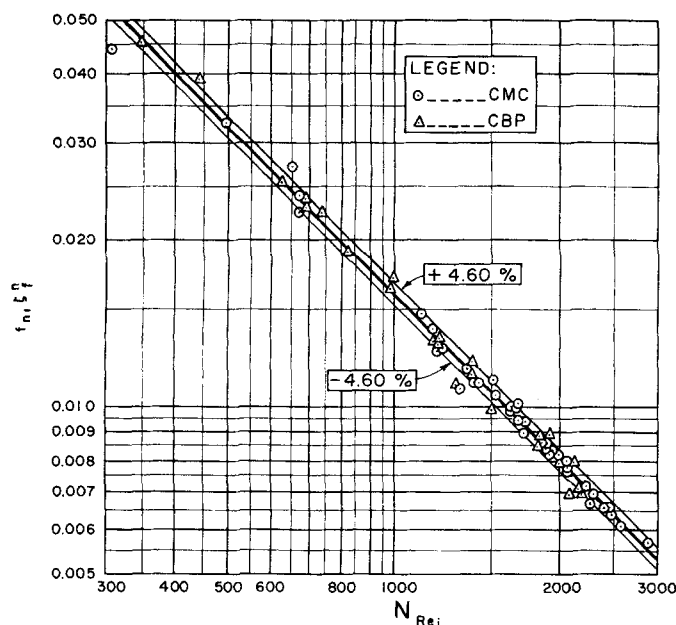


Fig. 8. Data of present investigation.

Introducing Equations (28) and (29) into Equation (10) one obtains $\zeta_i = \lambda(z)^{(1+3n)/n} +$

$$\frac{1 + 3n}{n\nu_o} [1 - \lambda(z)^{n*}] \exp [\Delta\phi] \quad (31)$$

where

$$\nu_o = \frac{1 + 3n}{n} \frac{\Delta\phi}{Ln\lambda(z)} \quad (32)$$

EXPERIMENTAL APPARATUS AND PROCEDURE

The system (illustrated in Figure 3) consisted of a 200-gal. reservoir tank, a 25-hp. progressing-cavity pump, an 80-gal. surge tank, and a double-pipe water cooler preceding the heating sections. The three test sections consisted of 1, 1½, and 2-in. iron pipe size copper pipes, each surrounded by two concentric steam jackets. The external jacket was supplied with steam at the same pressure as that in the internal jacket and thus served as an insulator to minimize heat losses. Each test section was preceded by 15 ft. of straight tubing which served as a calming section and was insulated to minimize heat losses and insure constancy of the inlet temperature.

Mass flow rates were determined by diverting the fluid stream into an oil drum mounted on a 1,000 lb. capacity platform scale and measuring the time required for the accumulation of 100 lb. of fluid.

Inlet and outlet temperatures were measured with 0° to 100°C. laboratory grade thermometers graduated in 0.1°C. increments. Wall temperatures were measured with a series of thermocouples placed at regular intervals along and around the pipes. The thermocouple readings were recorded continuously by a 12-point null-balance recording potentiometer. Small pressure drops were measured with a 50-in. water-carbon tetrachloride manometer, and large pressure drops were measured

with a 100-in. water-mercury manometer. Both manometer scales were graduated in 0.1-in. divisions.

The rheological properties of the solutions studied were determined with two viscometers, a rotational viscometer built by Salt (15) and modified by Stevens (16) and Craig (9), and a capillary viscometer built by Petersen (17).

When the steady state had been reached (all temperatures constant for at least 10 min.), the pressure drop and temperature data were recorded. Two mass flow rate determinations were made and the results averaged.

Viscometer samples were collected immediately before the first run of the day, at the end of the last run, and occasionally in the middle of the set of runs. These samples were tested immediately in one of the above mentioned viscometers.

The pseudoplastic fluids used in the present investigation were aqueous solutions of sodium carboxymethylcellulose (CMC) and carboxypolymethylene (CBP). It was found (9, 12, 17) that simultaneous heating and pumping of the fluids caused a slow but steady change in their rheological properties. Fortunately the change in fluid properties was slow enough that average values of the viscometer results could be used for several flow data points. No short term time-dependent changes (thixotropy) were observed.

Fluid density, heat capacity, and thermal conductivity were assumed to be identical with those of pure water, in agreement

TABLE 1. VALUES OF PARAMETERS FOR NUMERICAL INTEGRATION

n	$\Delta\phi$
2	0, 1, 2
1	0, 1, 2
3/4	0, 1, 2
6/10	0, 1
1/2	0, 1, 2
1/3	0, 1, 2

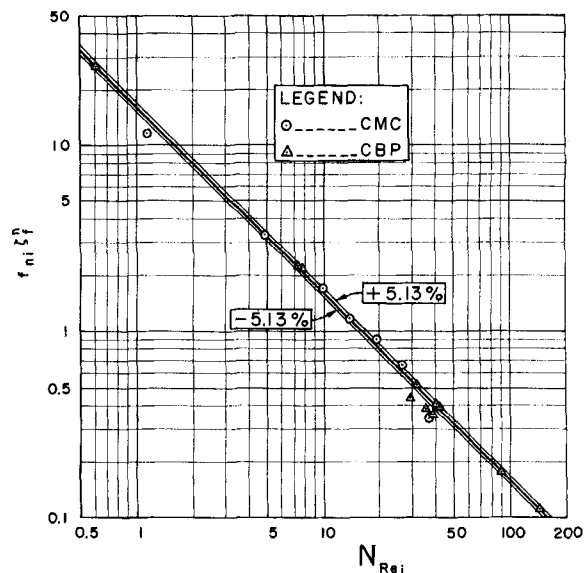


Fig. 9. Data of Vaughn.

with the experimental findings of Craig (9) and Mortenson (18).

COMPUTER RESULTS

Typical curves obtained by numerical integration of the conduction equation are illustrated in Figures 4 through 6. Each set of curves corresponds to a fixed value of n and is parameterized by $\Delta\phi$. Both of the above mentioned methods of computing the function ζ_i agree within less than 1%, thus showing that the approximate solution is sufficiently accurate for calculation purposes. A sample of the velocity profile curves mentioned above is shown in Figure 7. Curves were computed for each of the cases listed in Table 1.

EXPERIMENTAL RESULTS

Laminar flow data obtained for sixty-three different conditions are presented in Figure 8. The laminar flow data of Vaughn (19) are presented in Figure 9. The heavy straight line in both figures represents a rearrangement of Equations (16) through (18) into the form

$$f_{ni} \zeta_i^n = 16 N_{Re_i}^{-1} \quad (33)$$

The two light lines parallel to the heavy straight line described by Equation (33) represent the standard deviation of the data with respect to the Equation (33). This standard deviation is 4.6% for the data of the present investigation and 5.13% for Vaughn's data.

The data shown in Figure 8 cover a tenfold range of friction factors and pseudoplastic Reynolds numbers. Eighteen different fluids are represented with values of n ranging from 0.498 to 0.936 and values of $\Delta\phi$ from 0.527 to 1.630. These data were obtained in

all three diameter pipes with L/D values ranging from 28.8 to 228. There is no noticeable stratification of the data with respect to any of the above variables. The mean deviation of the experimental data from the theoretical line is within the precision of the data.

Vaughn's data (19), shown in Figure 9, appear to be the only laminar nonisothermal non-Newtonian flow data in the literature. These data, which Vaughn was unable to correlate successfully (19) by empirical means, are well correlated by Equation (33). Five of Vaughn's points (two CMC and three CBP) are significantly out of line with the remainder of his data. In view of the internal consistency of the other data points these five are suspected of being in error and were ignored in the statistical analysis. Vaughn obtained data for a third solution, but these data appear to involve a large error and were not considered further.

The data presented in Figures 8 and 9 cover a range of friction factors from 5.71×10^{-3} to 27.3 and a range of N_{Re} from 0.616 to 2,900. This is nearly a 5,000-fold variation. In addition the L/D ranged from 28.8 to 228, and the radial temperature difference ranged from 18.4° to 57.4°C . These data are correlated with an over-all standard deviation of 4.9%. The equations derived above may be used to predict nonisothermal friction factors from fundamental viscometer data and arbitrary pipe-flow system specifications.

In the derivation of the theoretical equations no limitation was placed on the type of fluids involved other than the applicability of the reduced Ostwald-deWaele or power law equation. There is therefore no a priori reason to assume that the theoretical results of this investigation may not be applied to the nonisothermal flow of dilatant fluids ($n > 1$) as long as the applicability of the specified rheology may be assumed. This assumption is in fact partially verified by the numerical solution to the conduction equation obtained for the case $n = 2$. This particular solution shows no great differences from those for n less than unity. Ideal Bingham plastic fluids have been explicitly excluded from the present treatment, since the yield stress of these fluids introduces additional complications not considered here.

ACKNOWLEDGMENT

The authors wish to express their gratitude to the Hercules Powder Company and the B. F. Goodrich Chemical Company who furnished the polymers used in the experimental part of this investigation. The authors are indebted to the Union Carbide Nuclear Company for supplying

the funds and part of the equipment which made the investigation possible. Finally, the authors wish to thank the University of Utah Computer Center for making their digital computer available for this work.

NOTATION

(Any consistent units may be used:
 m = mass, L = length, T = time,
 θ = temperature)

c	= heat capacity, ($L^2/T^2\theta$)
D	= tube diameter, (L)
E^\pm	= energy of activation per mole, (mL^2/T^2)
F	= computer function defined by Equation (26)
\bar{F}_b	= external body force in Equation of motion, (mL/T^2)
f	= Fanning friction factor, $g_{\rho}D\Delta p/2G^2L$, dimensionless
G	= mass flux, (m/TL^2)
g_c	= force unit conversion factor, (mL/T^2) (other force unit)
I_1, I_2	= integrals defined by Equations (22) and (23)
k	= thermal conductivity, ($mL/T^2\theta$)
k_p	= power law constant, (mT^{n-2}/L)
k_r	= constant defined by Equation (8), (mT^{n-2}/L)
L	= length of heater, (L)
N_{Gz}	= Graetz number, cLG/k , dimensionless
N'_{Gz}	= modified Graetz number, $\pi R_w^2 N_{Gz}/L^2$, dimensionless
N_{Re}	= pseudoplastic Reynolds number defined by Equation (18)
n	= power law exponent
$-\Delta p/L$	= axial pressure gradient, (m/L^2T^2)
Δp	= over-all pressure difference, (m/LT^2)
Q	= volumetric flow rate, (L^3/T)
R	= gas constant per mole, ($mL^2/T^2\theta$)
R_w	= tube radius, (L)
r	= radial coordinate, (L)
S'_r	= reduced shear rate defined by Equation (2), (T^{-1})
T	= absolute temperature, (θ)
T_i, T_w	= inlet and wall temperatures of fluids, (θ)
\bar{T}	= stress tensor in equation of motion, (m/LT^2)
t	= normalized temperature, $(T - T_i)/(T_w - T_i)$, dimensionless
u, v, w	= velocity components, (L/T)
\bar{u}	= velocity vector, (L/T)
\bar{v}	= area mean velocity, (L/T)
w	= mass flow rate, (m/T)
x	= normalized radial coordinate, r/R_w , dimensionless

Greek Letters

α	= numerical constant
Γ	= pseudo shear rate, $Q/\pi R_w^3$, (T^{-1})
δ_0	= intercept shown in Figure 1
$\Delta\phi$	= $\frac{E^\pm}{R} \left[\frac{1}{T_i} - \frac{1}{T_w} \right]$
$\bar{\nabla}u$	= strain-rate tensor, (T^{-1})
ζ_r	= nonisothermal flow function defined by Equation (10)
$\lambda(z)$	= function defined by Equation (30)
π	= 3.14159....
ρ	= density, (m/L^3)
τ	= shear stress, (m/LT^2)
τ_w	= wall shear stress, (m/LT^2)
$\phi(x, z)$	= $E^\pm/RT(x, z)$
ϕ_i	= E^\pm/RT_i
ϕ_w	= E^\pm/RT_w

Subscripts

ni	= nonisothermal
iso	= isothermal
i	= inlet
w	= wall

LITERATURE CITED

- Graetz, L., *Ann. d. Phys.*, **18**, 79 (1883); **25**, 337 (1885).
- Leveque, J., *Ann. mines (Ser. 12)*, **13**, 201, 305, 381 (1928).
- Lyche, B. C., and R. B. Bird, *Chem. Eng. Sci.*, **6**, 35 (1956).
- Pigford, R. L., *Chem. Eng. Progr. Symposium Ser. 17*, **51**, 79 (1955).
- Yablonskii, V. S., *Trudy Moskov. Neft. Inst.*, **17**, 3-42 (1956).
- Sieder, E. N., and G. E. Tate, *Ind. Eng. Chem.*, **28**, 1429 (1936).
- Rohanczi, G., *Eidg. Mater. prüf. u. Versuchsanstalt für Ind., Bauw., u. Gewerbe-Zurich*, Ber. 115, Zurich (1939).
- Petukhov, B. S., and G. F. Muchnik, *Zhurn. Tech. Phys.*, **27**, 1095 (1957).
- Craig, S. E., Jr., Ph.D. thesis, Univ. Utah, Salt Lake City, Utah (1959).
- Craig, S. E., Jr., and E. B. Christiansen, *A.I.Ch.E. Journal*, to be published.
- Metzner, A. B., and J. C. Reed, *A.I.Ch.E. Journal*, **1**, 434 (1955).
- Hanks, R. W., Ph.D. thesis, Univ. Utah, Salt Lake City, Utah (1960).
- Christiansen, E. B., N. W. Ryan, and W. E. Stevens, *A.I.Ch.E. Journal*, **1**, 544 (1955).
- Hildebrand, F. B., "Introduction to Numerical Analysis," McGraw-Hill, New York (1956).
- Salt, D. L., M.S. thesis, Univ. Utah, Salt Lake City, Utah (1949).
- Stevens, W. E., Ph.D. thesis, Univ. Utah, Salt Lake City, Utah (1952).
- Petersen, A. W., Ph.D. thesis, Univ. Utah, Salt Lake City, Utah (1960).
- Mortenson, Craig, B.S. thesis, Univ. Utah, Salt Lake City, Utah (1960).
- Vaughn, R. D., Ph.D. thesis, Univ. Delaware, Newark, Delaware (1956).

Manuscript received November 29, 1960; revision received March 27, 1961; paper accepted March 29, 1961. Paper presented at A.I.Ch.E. Tulsa meeting.